Hindawi
Security and Communication Networks
Volume 2023, Article ID 9831719, 1 page
https://doi.org/10.1155/2023/9831719

Retraction

Retracted: Parabolic Detection Algorithm of Tennis Serve Based on Video Image Analysis Technology

Security and Communication Networks

Received 26 December 2023; Accepted 26 December 2023; Published 29 December 2023

This article has been retracted by Hindawi, as publisher, following an investigation undertaken by the publisher [1]. This investigation has uncovered evidence of systematic manipulation of the publication and peer-review process. We cannot, therefore, vouch for the reliability or integrity of this article.

Please note that this notice is intended solely to alert readers that the peer-review process of this article has been compromised.

Wiley and Hindawi regret that the usual quality checks did not identify these issues before publication and have since put additional measures in place to safeguard research integrity.

We wish to credit our Research Integrity and Research Publishing teams and anonymous and named external researchers and research integrity experts for contributing to this investigation.

The corresponding author, as the representative of all authors, has been given the opportunity to register their agreement or disagreement to this retraction. We have kept a record of any response received.

References

[1] H. Tang, "Parabolic Detection Algorithm of Tennis Serve Based on Video Image Analysis Technology," *Security and Communication Networks*, vol. 2021, Article ID 7901677, 9 pages, 2021.

Hindawi
Security and Communication Networks
Volume 2021, Article ID 7901677, 9 pages
https://doi.org/10.1155/2021/7901677

Research Article

Parabolic Detection Algorithm of Tennis Serve Based on Video Image Analysis Technology

Hongxin Tang

Ministry of Sport and Military Affairs, China Ji Liang University, Hangzhou, Zhejiang 310018, China

Correspondence should be addressed to Hongxin Tang; thx027@cjlu.edu.cn

Received 3 September 2021; Revised 17 October 2021; Accepted 24 October 2021; Published 29 November 2021

Academic Editor: Jian Su

At present, the existing algorithm for detecting the parabola of tennis serves neglects the pre-estimation of the global motion information of tennis balls, which leads to great error and low recognition rate. Therefore, a new algorithm for detecting the parabola of tennis service based on video image analysis is proposed. The global motion information is estimated in advance, and the motion feature of the target is extracted. A tennis appearance model is established by sparse representation, and the data of high-resolution tennis flight appearance model are processed by data fusion technology to track the parabolic trajectory. Based on the analysis of the characteristics of the serve mechanics, according to the nonlinear transformation of the parabolic trajectory state vector, the parabolic trajectory starting point is determined, the parabolic trajectory is obtained, and the detection algorithm of the parabolic service is designed. Experimental results show that compared with the other two algorithms, the algorithm designed in this paper can recognize the trajectory of the parabola at different stages, and the detection accuracy of the parabola is higher in the three-dimensional space of the tennis service.

1. Introduction

With the development of the economy, tennis has become more and more popular in China. Every year, several large-scale tennis matches (professional and amateur) are held in each province, especially amateur matches. Serving is one of the most important techniques in modern tennis [1]. Serving is not only the beginning of a game, but also the only process of hitting that is controlled by oneself and not controlled by the opponent. Excellent serve can not only score directly, but also exert greater personal technical characteristics to control the opponent and maximize tactical intent. From the point of view of system theory, tennis service not only refers to the technical layer but also includes the tactical layer, psychological layer, and physical layer. Technical, tactical, psychological, and physical dimensions are interrelated, interdependent, and indivisible as a whole [2]. Parabolic trajectory is also the direct factor that affects the result of tennis match. Therefore, it is necessary to track and detect the parabolic trajectory of tennis service.

Fu and Guan [3] proposed a particle filter tennis motion tracking method based on Kalman filter prediction. Based on the excellent localization characteristics of multi-scale wavelet transform in time domain and space domain, the adjacent video images are differentiated to extract the target feature information reflecting the foreground motion, so as to overcome the adverse factors of illumination change and tennis motion scale changing with time. At the same time, based on the structural characteristics of tennis court, the influence of adverse interference factors outside the court is excluded. On this basis, the Kalman filter is used to predict and modify the particles, integrate the current observation information into the particle filter process, estimate the mean and covariance of the predicted particle state, make the

dynamic particles closer to the posterior probability distribution, and improve the tracking accuracy of tennis moving target. Hua et al. [4] proposed an improved multi-target detection framework LSTM-SSD, which is dedicated to traffic scene video multi-target detection. The single image detection framework is combined with recurrent neural network and LSTM network to form an interleaved cyclic convolution structure. By using a bottleneck LSTM layer to extract the feature mapping between propagation frames, the temporal correlation of network frame level information is realized, which greatly reduces the network computing cost. Combining the time perception information with the improved dynamic Kalman filter algorithm, the tracking and recognition of targets affected by strong interference such as illumination change and large-area occlusion in video is realized.

However, the above two traditional methods ignore the pre-estimation of the global motion information of tennis, resulting in low accuracy of serve parabolic detection results and unsatisfactory trajectory recognition rate in different directions. Therefore, a tennis serve parabolic detection algorithm based on video image analysis technology is proposed.

Our contribution is threefold:

(1) At present, the existing algorithm for detecting the parabola of tennis serves neglects the pre-estimation of the global motion information of tennis balls, which leads to great error and low recognition rate. Therefore, a new algorithm for detecting the parabola of tennis service based on video image analysis is proposed.

(2) A tennis appearance model is established by sparse representation, and the data of high-resolution tennis flight appearance model are processed by data fusion technology to track the parabolic trajectory.

(3) Based on the analysis of the characteristics of the serve mechanics, according to the nonlinear transformation of the parabolic trajectory state vector, the parabolic trajectory starting point is determined, the parabolic trajectory is obtained, and the detection algorithm of the parabolic service is designed.

The remainder of this paper is organized as follows. Section 2 introduces the construction of parabolic trajectory tracking model for tennis serve. Section 3 discusses the parabolic detection algorithm for tennis serve. Section 4 discusses experiment and analysis. Section 5 presents the conclusions of the study.

2. Construction of Parabolic Trajectory Tracking Model for Tennis Serve

2.1. Video Target Motion Feature Extraction. In order to obtain the complete semantic information of the video moving target, the local motion features of targets in the video image are extracted to ensure the effective behavior recognition of subsequent video targets [5, 6]. In order to extract the local motion information of video object effectively, the global motion information must be estimated in advance, and the global motion information must be eliminated when analyzing the local target motion [7]. In this paper, a fast diamond search and matching method is used to perform the global motion extraction, and then the local dense motion vector field is deduced by optical flow analysis.

The basic concept of optical flow field is to take the moving image function $f(x, y, z)$ as a continuous function of variables x, y, and z. In the case of period $t + \Delta t$, the point moves to a new position, the orientation in the image becomes $(x + \Delta x, y + \Delta y)$, and the gray value is $f(x + \Delta x, y + \Delta y, z + \Delta z)$. The optical flow convergence formula is constructed according to the image gray conservation theorem, and the following results are obtained:

$$f(x, y, z) = f(x + \Delta x, y + \Delta y, z + \Delta z). \tag{1}$$

Extend the right side of the equation using Taylor's formula:

$$f(x, y, z) = f(x, y, z) + \frac{\partial f(x, y, z)}{\partial x}\Delta x + \frac{\partial f(x, y, z)}{\partial y}\Delta y + \frac{\partial f(x, y, z)}{\partial t} + \Delta z + e, \tag{2}$$

$$u(x, y, z) = \frac{\Delta x}{\Delta t}, v(x, y, z) = \frac{\Delta y}{\Delta t}. \tag{3}$$

Assuming that equation (3) is true, the relationship shown in equation (4) can be obtained.

$$\frac{\partial f(x, y, z)}{\partial x} + \frac{\partial f(x, y, z)}{\partial y} + \frac{\partial f(x, y, z)}{\partial z} = 0. \tag{4}$$

Since ∇f is the gradient of pixel (x, y), equation (4) can be reduced to

$$\frac{\partial f}{\partial t} = -\nabla f \cdot (u, v), \tag{5}$$

where (u, v) represents the motion vector of pixel (x, y) in period t. Equation (5) is the optical flow convergence formula.

The optical flow field caused by the same moving object should have the characteristics of continuity and smoothness, that is, if the rate of adjacent points in the same object is the same, the optical flow change projected onto the image should also be smooth [8, 9]. According to this characteristic, an additional convergence condition added to the optical flow field is designed in this paper:

$$\min G = \left(\frac{\partial u}{\partial x}\right)^2 + \left(\frac{\partial u}{\partial y}\right)^2 + \left(\frac{\partial v}{\partial x}\right)^2 + \left(\frac{\partial v}{\partial y}\right)^2. \quad (6)$$

It can be seen from the above formula that the global smooth convergence can transform the optical flow field operation problem into an optimization problem. Replace the optical flow deviation and rate field gradient deviation [10] in equation (6) and record the two deviations as

$$e' = \frac{\partial f}{\partial x}u + \frac{\partial f}{\partial y}v + \frac{\partial f}{\partial t}. \quad (7)$$

2.2. Appearance Model Based on Sparse Representation. Based on the sparse representation model, the appearance model of flying tennis was constructed by using the target feature extraction algorithm [11]. When extracting the features of tennis flight image, the local preserving mapping algorithm is used to reduce the dimension of tennis flight image data while retaining the original data features.

In the feature extraction of tennis flight image, firstly, the K-nearest neighbor method is used to construct the interclass adjacency graph and intraclass adjacency graph [12, 13].

Then, determine the edge weight. The algorithm used is as follows:

$$S_{i,j} = \begin{cases} 1 & x_i \text{ and } x_j \text{ are neighbors to each other} \\ 0 & \text{otherwise} \end{cases}, \quad (8)$$

where $S_{i,j}$ represents the weight on the edge and x_i and x_j represent the edges of tennis flight image features, respectively.

Then, build a flying tennis appearance model based on the sparse representation model, that is, build a flying tennis appearance model through a sparse reconstruction algorithm. The specific build process for the appearance model is as follows:

(1) Input the features of tennis flight images and train the dictionary pairs with higher resolution and lower resolution, which are represented by $\{H_1, H_2\}$ and $\{U_1, U_2\}_{k=1}^{N}$.

(2) For each image block Y_iC (size is $b \times b$) in the tennis flight image Y, each image block is processed sequentially from the image block in the upper left corner.

(3) Calculate the Y_i-means.

(4) Extract the feature block of Y_i.

(5) Calculate dictionaries $\mathrm{vec}(Z_i)$ and H as follows:

$$\mathrm{vec}(Z_i) = \begin{bmatrix} \mathrm{vec}(\widetilde{X}_i) \\ \mathrm{vec}\left(F^{(1)}Y_i\right) \\ \vdots \\ \mathrm{vec}\left(F^{(k)}Y_i\right) \\ \vdots \\ \mathrm{vec}\left(F^{(N)}Y_i\right) \end{bmatrix}, \quad (9)$$

$$H = \begin{bmatrix} H_2^h \otimes H_1^h \\ U_2^{(1)} \otimes U_1^{(1)} \\ \vdots \\ U_2^{(k)} \otimes U_1^{(k)} \\ \vdots \\ U_2^{(N)} \otimes U_1^{(N)} \end{bmatrix}, \quad (10)$$

where $\widetilde{X}_i$ represents the reconstructed high-resolution tennis flight image of the reconstructed area.

(6) Build the image block of high-resolution tennis flight appearance model, as shown in the following formula:

$$X_i = \frac{B_i^T}{H_1^h \cdot U_2^{hT}}, \quad (11)$$

where X_i represents the constructed high-resolution tennis flight appearance model image block and T represents the sparsity balance parameter.

The repeated operation of partial weighted average is implemented on the image block of high-resolution tennis flight appearance model to construct high-resolution tennis flight appearance model X_0.

(7) Output the high-resolution tennis flight appearance model X_0.

2.3. Establishing Tracking Algorithm Model. Firstly, the data of high-resolution tennis flight appearance model are processed by data fusion technology [14, 15]. The data fusion algorithm used is D-S evidence theory, which mainly divides the evidence set into multiple irrelevant parts, independently judges the identification framework through the divided parts, and then recombines these parts through Dempster rules. The specific combination rules are as follows:

$$\begin{cases} Z = \dfrac{m_1(A_i)m_2\left(B_j\right)}{k} \cdot A \neq 0,\ m(\phi) = 0 \\ A_i \cap B_j = A \end{cases}, \quad (12)$$

where A_i and B_j, respectively, represent two independent evidence sources; A stands for proposition; $m(\phi)$ represents the universe set of trust functions; m represents trust function; and k stands for the number of propositions.

Then, the parabolic trajectory tracking model of tennis serve is constructed by particle filter algorithm [16, 17]. In the model construction, the measurement covariance has an important impact on the final filter output. In order to avoid the influence of measurement covariance, dynamic correction is introduced, as shown in the following formula:

$$R_k = V(I), \tag{13}$$

where R_k represents the measurement covariance; $V(\cdot)$ represents the dynamic correction function; and I represents the distance between the binocular camera and the tennis ball at a certain time in the three-dimensional space, that is, the parabolic trajectory tracking algorithm model of tennis ball serving, as shown in the following formula:

$$d_k = \sqrt{(x_k - x_c)^2 + (y_k - y_c)^2 + (z_k - z_c)^2}, \tag{14}$$

where x_k, y_k, and z_k represents the coordinate measurement value of the tennis ball flying in the three-dimensional world coordinate system; x_c, y_c, and z represent the midpoint position when the two optical centers are connected with the left and right cameras.

3. Parabolic Detection Algorithm for Tennis Serve

3.1. Stress Analysis of Tennis. When analyzing the force on a tennis ball, firstly, the rotating axis of the tennis ball is defined, and the object of the study is a certain state of the tennis ball stagnating in the parabolic trajectory of the actual service. Combined with the flow velocity of air during the course of the tennis ball rotation, the coordinate system is established as follows. The Z axis of the rotating tennis ball is the coordinate system, and the force coordinate system shown in Figure 1 is obtained.

From the tennis coordinate system established in Figure 1, the velocity of the tennis is set to the X axis, and the pressure on the tennis is set to the Y axis. According to the direction of the coordinate system, it can be analyzed that the tennis ball is mainly affected by gravity, air resistance, and Magnus force in the air. Define time t of the tennis ball shown in Figure 1 above. The speed of the tennis ball is

$$v(t) = \left[v_x(t), v_y(t), v_z(t)\right]^T, \tag{15}$$

where T represents the flight time of the tennis ball and $v_x(t), v_y(t), v_z(t)$ represent the movement speeds in different axes, respectively. Then, the rotation angular velocity of the tennis ball is calculated, and the calculation formula is

$$W = \left[\omega_x, \omega_y, \omega_z\right]^T, \tag{16}$$

where $\omega_x, \omega_y, \omega_z$, respectively, represent the angular velocities of tennis balls in different axes. Based on the above values of angular velocity and rotation speed, the gravity, air resistance, and MAG effort of the tennis ball at that time are calculated:

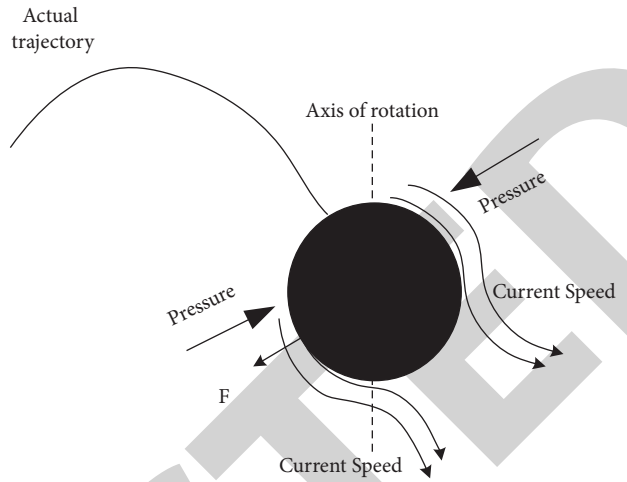

Figure 1: Tennis coordinate system established.

$$\begin{cases} Fg = -m\begin{bmatrix} 0 & 0 & g \end{bmatrix}^T \\ Fa = \dfrac{1}{2} C_d \rho A |v(t)| \\ Fm = \dfrac{1}{2} C_m \rho r A |W \times v(t)| \end{cases}, \tag{17}$$

where m is the weight of the tennis ball, g is the gravitational acceleration, C_d is the air resistance coefficient, C_m is the Magnus force coefficient, ρ is the air density under the standard air pressure, A is the cross-sectional area of the tennis ball, r is the radius of the tennis ball, and the meaning of other parameters remains unchanged.

From the above formula, we can see that the air resistance is proportional to the square of the speed of the tennis. When the speed of one side of the tennis ball is not parallel to the direction of the spin speed, under the action of air on one side of the tennis ball, the superposition of the flying speed and the spin speed becomes larger, and the speed of the other side of the tennis ball is offset by the action of air. The parabolic trajectory of the serve is to track the tennis movement process obtained by the force analysis above and, finally, obtain the parabolic trajectory and mechanical analysis of different tennis balls.

3.2. Parabolic Trajectory Detection of Tennis Serve. Under the tennis motion expression obtained from the above analysis, the tennis stop rotation process is defined to represent the end of the iterative process, and the noise generated by the iterative process is calculated. The calculation formula is

$$K = \frac{1}{2\pi} \cdot \frac{\rho}{m} \cdot C \cdot D^3, \tag{18}$$

where C represents the lift coefficient, D represents the diameter of the tennis ball, and the meaning of other parameters remains unchanged. Under the influence of the above noise value, predict the state vector of the tennis ball and take the above calculated noise value as a priori

estimation value, and the state vector can be expressed as [18, 19]

$$\begin{cases} X_{(k|k-1)} = F\left(X_{k-1}, U_{k-1}\right) \\ P_{(k|k-1)} = A_{k-1}P(k-1) + Q_k \end{cases}, \quad (19)$$

where $X_{(k|k-1)}$ represents a priori estimated value of tennis state variable, $P_{(k|k-1)}$ represents a priori estimated value of covariance of state variable, A_k represents partial derivative of motion process function F to state variable, and Q_k represents noise vector. According to the above state vector values, the number of state data of different tennis balls is divided, as shown in Table 1.

3.3. Parabolic Trajectory Acquisition of Tennis Serve. According to the nonlinear transformed state vector of the serving parabolic trajectory, the starting point of the serving parabolic trajectory is determined. In order to simplify the calculation process in the tracking process of the serving parabolic trajectory, the distribution distance is regarded as a constant, and the force on the tennis ball can be expressed as

$$F_{\text{total}} = F\left(t, \kappa^{(k)}\right)^2, \quad (20)$$

where $\kappa^{(k)}$ represents the level parameter of class in the process of continuous sampling motion. According to the tracking results of the above collection points, the coordinates of the tennis ball at the sampling point are determined, and the coordinate values of the collection points are summarized as shown in Table 2.

The coordinates of the tennis ball in three directions shown in Table 2 are taken as the parabolic trajectory dataset, the coordinate values in the above table are processed by nonlinear filtering, and the parabolic trajectory of the tennis ball is continuously updated. The update expression is as follows:

$$K_n = \frac{F}{S_x S_y S_z \cos\theta}, \quad (21)$$

where S_x, S_y, and S_z represent the values of three axes, respectively, and θ represents the included angle between the parabolic trajectory of the actual tennis serve and the three axes. According to the calculation formula of sampling points formed by the above integration, the parabolic trajectory of tennis serve is simulated in a three-dimensional coordinate, as shown in Figure 2.

As shown in Figure 2, the projectile trajectories of different tennis balls in tennis sports are finally studied on the premise of mechanical analysis.

4. Analysis of Experimental Results

4.1. Tennis Parabolic Motion Recognition Rate. In the experiment, the flying image of the robot tennis ball is collected, and the image is processed in a series of ways, which is used to detect the trajectory of the tennis ball in the experiment. Experimental images are shown in Figure 3.

In order to verify the effectiveness of the algorithm in this paper, the algorithm in this paper, the tennis moving target tracking algorithm based on Kalman predictive particle filter proposed in literature [3], and the identification results of different stages of tennis projectile motion by video multi-target detection technology based on recursive neural network proposed in literature [4] are tested successively, as shown in Figure 4.

Table 1: Data vectors in different rotation states.

Serial number	Rotation attribute	Output data vector
1	Internal rotation	04
2	External rotation	01
3	Irrotational	07

Figure 4 shows that the tennis parabolic motion recognition result generated by this algorithm is better than the other two documents. This is because the algorithm fully considers the use of camera calibration in the process of generating the neutral parabolic trajectory and the target dynamic analysis of the neutrality of the target motion state parabolic trajectory to improve the accuracy of video action recognition.

4.2. Parabolic Trajectory Tracking Results of Tennis Serve in X, Y, and Z Directions

4.2.1. X-Axis Test Results. Using the designed tennis serve parabolic trajectory detection algorithm, the serve parabolic trajectory of tennis thrown by the experimental tennis robot is tracked. In the tracking, the parabolic trajectory detection of tennis serve is tested from three angles of X axis, Y axis, and Z axis. The test results of parabolic trajectory detection of tennis serve on X axis are shown in Figure 5.

From the X-axis tennis serve parabolic trajectory detection experimental results in Figure 5, it can be seen that there is almost no significant difference between the tennis serve parabolic trajectory detection output and the actual flight serve parabolic trajectory of tennis. With the passage of time, the tracking result of the design algorithm is still relatively stable and the output noise is small, which proves that the detection effect of X-axis tennis serve parabolic trajectory of the design algorithm is better.

4.2.2. Y-Axis Test Results. Then, the parabolic trajectory of the Y-axis tennis service is tested, and the test results are shown in Figure 6.

Based on the detection of the parabolic trajectory of the Y-axis tennis service in Figure 6, it is found that the algorithm based on data fusion and sparse representation model can track the Y axis accurately in 3D world coordinate system. It is proved that the designed algorithm can detect the parabolic trajectory of the Y-axis service with high precision because the result is very close to the reality.

4.2.3. Z-Axis Test Results. Finally, the Z-axis tennis serve parabolic trajectory detection of the designed algorithm is tested, and the specific test results are shown in Figure 7.

From the parabolic trajectory detection of the Z-axis tennis ball in Figure 7, we can see that the accuracy of the

Table 2: Collection point coordinates of parabolic trajectory of tennis serve.

Collection point name	X-axis value (m)	Y-axis value (m)	Z-axis value (m)
1	7.135	1.188	0.393
2	7.322	1.093	4.204
3	3.716	1.918	0.773
4	4.237	0.399	2.721
7	4.184	9.701	1.038
3	2.349	8.033	3.793
7	4.012	7.193	7.318
8	4.405	3.301	9.787
9	7.379	7.421	3.728
10	0.274	7.072	1.029
11	3.198	2.028	2.707
12	7.192	9.322	7.823
13	8.915	7.079	2.002
14	7.316	0.773	0.724
17	7.748	3.133	1.373
13	3.483	2.873	3.819
17	7.197	3.703	7.729
18	7.139	8.341	7.818
19	7.279	9.308	4.878
20	7.707	7.877	7.897

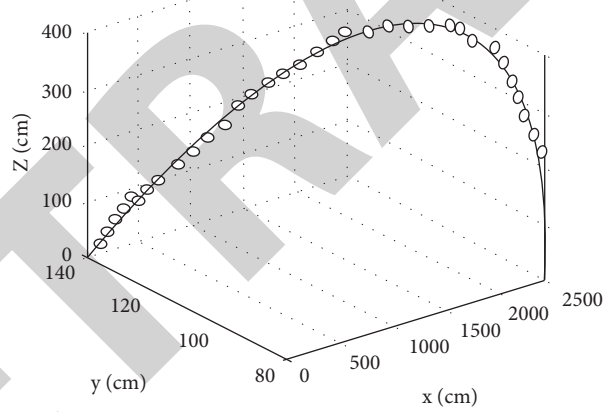

Figure 2: Projectile trajectory of a tennis serve.

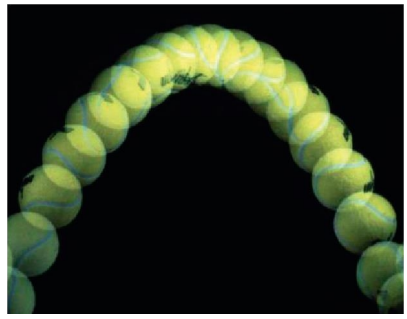

Figure 3: Tennis projectile motion simulation diagram.

parabolic trajectory tracking of the Z-axis tennis ball is lower than that of the X-axis and Y-axis tennis ball, and the whole parabolic trajectory tracking has some errors, but the accuracy is still high.

Combining the detection results of the three direction axes, it can be found that the output of the tennis serve parabolic detection algorithm is very close to the reality, that is, the designed tennis serve parabolic trajectory tracking

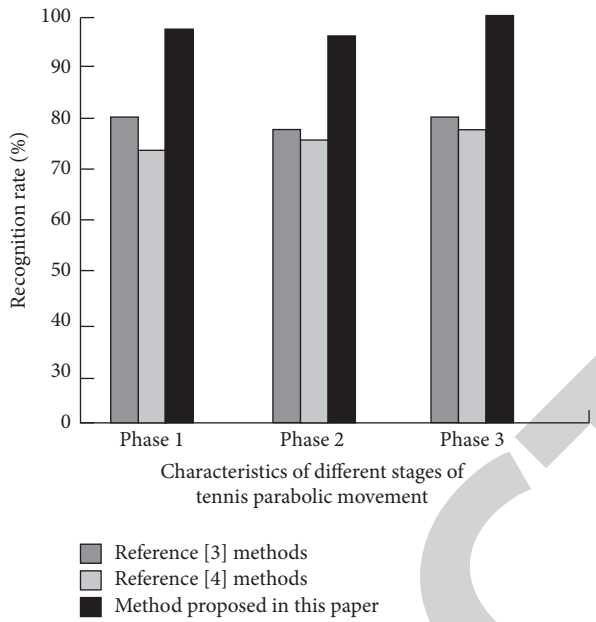

Figure 4: Comparison of recognition rates of different algorithms in different stages of tennis projectile motion.

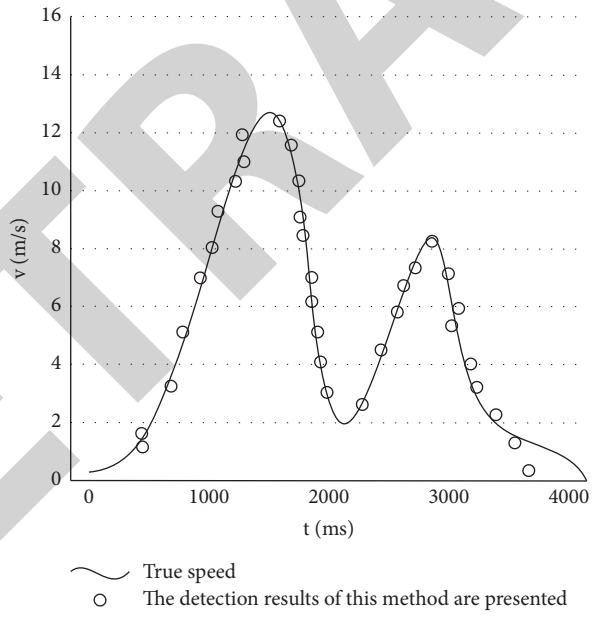

Figure 5: Test results of parabolic trajectory detection of tennis serve on X axis.

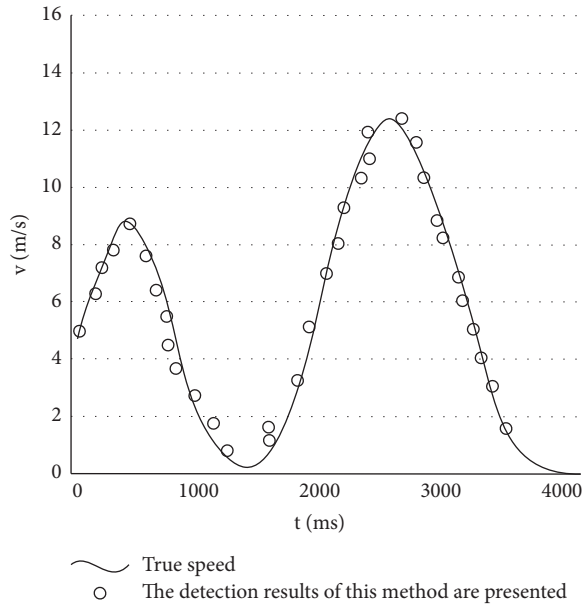

Figure 6: Parabolic trajectory detection of *Y*-axis tennis serve.

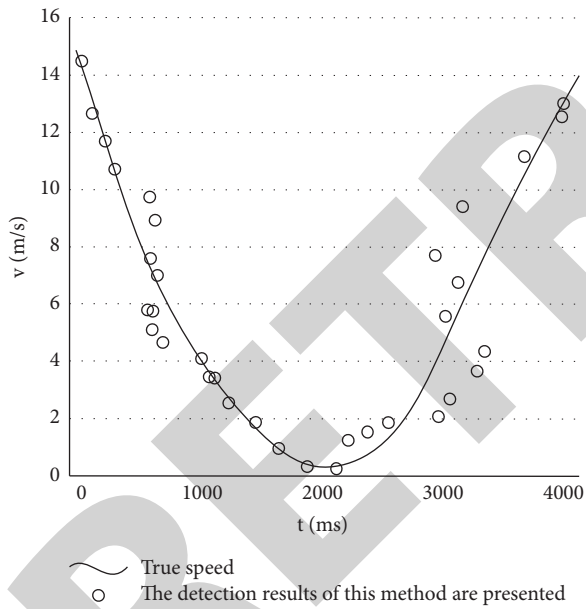

Figure 7: Parabolic trajectory detection of *Z*-axis tennis serve.

algorithm based on data fusion and sparse representation model can detect the tennis serve parabolic trajectory more accurately.

5. Conclusion

In order to solve the problem that the traditional algorithm for detecting the parabola of tennis serve cannot track the track of the ball in different directions, a new algorithm based on video image analysis is proposed. Through sparse representation and data fusion technology, the high-resolution tennis flying appearance model data are processed and the parabolic trajectory of tennis serve is tracked. We determine the starting point of the parabolic trajectory and complete the parabolic testing of the tennis service. Experimental results show that the proposed algorithm can identify the trajectory of tennis service parabola in different stages with high accuracy, which provides a reliable theoretical support for further research.

Data Availability

The data used to support the findings of this study are available from the corresponding author upon request.

Conflicts of Interest

The author declares that there are no conflicts of interest.

References

[1] Y. Wang and M. Wen, "Simulation of tennis match scene classification algorithm based on adaptive Gaussian mixture model parameter estimation," *Complexity*, vol. 2021, no. 1, 12 pages, Article ID 3563077, 2021.

[2] V. Moreno-Pérez, Á. López-Samanes, R. Domínguez et al., "Acute effects of a single tennis match on passive shoulder rotation range of motion, isometric strength and serve speed in professional tennis players," *PLoS ONE*, vol. 14, no. 4, pp. e0215015–e0215026, 2019.

[3] R. Fu and Y. P. Guan, "Tennis motion tracking based on particle filter in kalman filter prediction," *Chinese Journal of Electron Devices*, vol. 42, no. 4, pp. 167–171, 2019.

[4] X. Hua, X. Q. Wang, and Z. Y. Ma, "Video multi-target detection technology based on recursive neural network," *Application Research of Computers*, vol. 37, no. 2, pp. 301–306, 2020.

[5] W. Sun, D. Yan, J. Huang, and S. Changhao, "Small-scale moving target detection in aerial image by deep inverse reinforcement learning," *Soft Computing*, vol. 24, no. 11, pp. 1–12, 2019.

[6] B. Pandey, S. Thakur, H. Joshi, and A. Pradhanga, "Towards video based collective motionanalysis through shape tracking andmatching," *Electronics Letters*, vol. 56, no. 17, pp. 2157–2168, 2020.

[7] A. Yuan, X. Li, and X. Lu, "3G structure for image caption generation," *Neurocomputing*, vol. 330, no. FEB.22, pp. 17–28, 2019.

[8] M. Meem, A. Majumder, and R. Menon, "Multi-plane, multi-band image projection via broadband diffractive optics," *Applied Optics*, vol. 59, no. 1, p. 38, 2020.

[9] G. Kertész, S. Szénási, and Z. Vámossy, "Comparative analysis of image projection-based descriptors in siamese neural networks," *Advances in Engineering Software*, vol. 154, no. 6, Article ID 102963, 2021.

[10] X. Li, X. Yang, S. Chen, N. Qi, and Y. Huang, "Intensity image quality assessment based on multiscale gradient magnitude similarity deviation," *Optical Engineering*, vol. 59, no. 10, pp. 452–463, 2020.

[11] W. Zhou, Y. Zhou, W. Qiu, T. Luo, and Z. Zhai, "Perceived quality measurement of stereoscopic 3D images based on sparse representation and binocular combination," *Digital Signal Processing*, vol. 93, pp. 128–137, 2019.

[12] N. R. Zhou, X. X. Liu, Y. L. Chen, and N. Du, "Quantum K-nearest-neighbor image classification algorithm based on

K-L transform," *International Journal of Theoretical Physics*, vol. 60, no. 4, pp. 1–16, 2021.

[13] P. Yingxia, Z. Xinyi, C. Guangqing et al., "Design and implementation of a parallel geographically weighted k -nearest neighbor classifier," *Computers & Geosciences*, vol. 127, pp. 111–122, 2019.

[14] G. Lei, R. Yao, Y. Zhao, and Y. Zheng, "Detection and modeling of unstructured roads in forest areas based on visual-2D lidar data fusion," *Forests*, vol. 12, no. 7, p. 820, 2021.

[15] N. Ghosh, R. Paul, S. Maity, K. Maity, and S. Saha, "Fault Matters: sensor data fusion for detection of faults using dempster-shafer theory of evidence in IoT-based applications," *Expert Systems with Applications*, vol. 162, no. 4, Article ID 113887, 2020.

[16] Y. Guo, "Moving target localization in sports image sequence based on optimized particle filter hybrid tracking algorithm," *Complexity*, vol. 2021, no. 7, 11 pages, Article ID 2643690, 2021.

[17] K. R. Mathusoothana, "Robust multi-view videos face recognition based on particle filter with immune genetic algorithm," *IET Image Processing*, vol. 13, no. 4, pp. 600–606, 2019.

[18] A. Nicolson and K. K. Paliwal, "Spectral distortion level resulting in a just-noticeable difference between ana prior-isignal-to-noise ratio estimate and its instantaneous case," *Journal of the Acoustical Society of America*, vol. 148, no. 4, pp. 1879–1889, 2020.

[19] Y. Feng, H. Wang, and Z. G. Qu, "Trajectory simulation of hypersonic gliding vehicle based on reference ellipsoid," *Computer Simulation*, vol. 37, no. 10, pp. 18–23, 2020.